Continuum Mech. Thermodyn. (2014) 26:67–78
DOI 10.1007/s00161-013-0290-0

ORIGINAL ARTICLE

Hassan Akhlaghi · Ehsan Roohi

Mass flow rate prediction of pressure–temperature-driven gas flows through micro/nanoscale channels

Received: 15 August 2012 / Accepted: 8 January 2013 / Published online: 1 February 2013

Abstract In this paper, we study mass flow rate of rarefied gas flow through micro/nanoscale channels under simultaneous thermal and pressure gradients using the direct simulation Monte Carlo (DSMC) method. We first compare our DSMC solutions for mass flow rate of pure temperature-driven flow with those of Boltzmann-Krook-Walender equation and Bhatnagar-Gross-Krook solutions. Then, we focus on pressure–temperature-driven flows. The effects of different parameters such as flow rarefaction, channel pressure ratio, wall temperature gradient and flow bulk temperature on the thermal mass flow rate of the pressure–temperature-driven flow are examined. Based on our analysis, we propose a correlated relation that expresses normalized mass flow rate increment due to thermal creep as a function of flow rarefaction, normalized wall temperature gradient and pressure ratio over a wide range of Knudsen number. We examine our predictive relation by simulation of pressure-driven flows under uniform wall heat flux (UWH) boundary condition. Walls under UWH condition have non-uniform temperature distribution, that is, thermal creep effects exist. Our investigation shows that developed analytical relation could predict mass flow rate of rarefied pressure-driven gas flows under UWH condition at early transition regime, that is, up to Knudsen numbers of 0.5.

Keywords DSMC · Thermal creep effects · Mass flow rate · Micro/nanochannel · Pressure–temperature-driven flows

1 Introduction

With the fast progress in micro/nanoscale devices and components, it is desired to obtain fundamental understanding of the transport phenomena in these devices. Additionally, a true understanding of the hydrodynamics and thermal physics of rarefied gas flows is crucial in design, fabrication and operation of micro/nano-electromechanical systems (MEMS/NEMS) [1,2]. Once the gas flow rarefies, the Knudsen number, defined as the ratio of gas mean free path to the characteristic length of the geometry, $\mathrm{Kn} = \lambda/\mathrm{H}$, increases and the flow analysis should be performed using accurate approaches based on the solution of the Boltzmann equation [3]. Due to the complexity of the direct solution of the Boltzmann equation, there are a wide set of alternative approaches for solution of this equation. Among different approaches, discrete molecular modeling of direct

Communicated by Andreas Ãchsner.

H. Akhlaghi · E. Roohi (✉)
High Performance Computing (HPC) Laboratory,
Department of Mechanical Engineering, Ferdowsi University of Mashhad, P.O. Box 91775-1111, Mashhad, Iran
E-mail: e.roohi@um.ac.ir
Tel.: +98-511-8805136
Fax: +98-511-8763304

H. Akhlaghi
E-mail: akhlaghi@alum.sharif.edu

simulation Monte Carlo (DSMC) is a key tool to model flow field in all degrees of rarefaction [4]. In DSMC, the gas is modeled as a collection of moving particles which interact through collisions. DSMC is known as one of the most successful particle simulation methods in analyzing the rarefied gaseous flows.

Pressure–temperature-driven flows may be considered to control mass and energy flow rates in micro/nanochannels [5]. This physics is also employed in Knudsen pumps. Knudsen pumps operate based on the thermal creep/transpiration flow due to non-uniform wall temperature distribution. These devices are employed in MEMS/NEMS, that is, micro/nanoscale Knudsen pumps are essential for the realization of completely miniaturized devices such as gas sensors, fuel cells and lab-on-a-chip systems [6–9]. Consequently, study of this class of micro/nano flows would be crucial for accurate design of MEMS/NEMS. There are continuing attempts for mass flow rate prediction of pressure–temperature-driven rarefied gas flows through micro/nanoscale channels. In addition to pressure gradient, wall temperature gradient may generate mass flow rate at micro/nanoscale. Thermal creep flows in gases occur by non-uniform temperature distributions in the flow boundaries [10]. In this situation, fluid starts creeping from the cold region toward the hot one. The thickness of the creep layer is proportional to the Knudsen number. Knudsen showed the pumping effect in thermal creep flows using experimental observations [11,12]. Thermal creep/transpiration problem is investigated by several authors using kinetic models of the Boltzmann equation. The flow between two parallel plates, where a constant unidirectional temperature gradient is applied to the plates, is a common flow configuration which is used in kinetic approaches. Loyalka et al. [13–17] presented kinetic theory analysis of thermal transpiration and mechanocaloric effects. They presented a general kinetic theory analysis and showed that the cross phenomena of thermal transpiration and mechanocaloric effect can be treated by the use of the variational technique for all rarefactions regimes. Kanki and Iuchi [18] investigated Poiseuille flow and thermal creep of a rarefied gas between two parallel plates using the Bhatnagar-Gross-Krook (BGK) model. They showed that the ratio of the flow rate of the thermal creep to that of the Poiseuille flow reduces to zero at the continuum flow limit and approaches to 0.5 as the density of the gas approaches to zero. Ohwada et al. [19] studied the Poiseuille and thermal transpiration flows of a rarefied gas between two parallel plates on the basis of the linearized Boltzmann equation for hard-sphere molecules. They predicted the mass fluxes of the Poiseuille and the thermal transpiration flows for the whole range of the Knudsen number with good accuracy compared to the existing numerical method and experimental results. They showed that in spite of the Poiseuille flow, mass flux increases continuously in thermal transpiration flow versus the Knudsen number. Alexeenko et al. [7] numerically investigated the temperature-driven gas flows in a two-dimensional finite length microchannel and a cylindrical tube using DSMC method, a discrete ordinate method for the ellipsoidal statistical model and BGK model. They examined the effects of various wall temperature distributions and compared different numerical methods. Taheri and Struchtrup [5] applied a streamwise constant temperature gradient over the walls of a microchannel and studied rarefied gas flow through the channel using fully linearized and semi-linearized forms of the regularized 13-moment (R13) equations.

The main objective of the current study is the mass flow rate prediction of the rarefied gas flow through micro/nanoscale channels under both of temperature and of pressure gradients over a wide range of Knudsen numbers. We will derive a predictive relation for mass flow rate of this class of flows. Subsequently, we will evaluate our relation with simulation results of channel flow under specified wall heat flux and uniform wall temperature boundary conditions. We use DSMC method as our direct simulation strategy.

2 DSMC method

DSMC is a numerical tool to solve the Boltzmann equation based on the direct statistical simulation of the molecular processes described by the kinetic theory [4]. The primary principle of DSMC is decoupling of the motion and collision for all simulated particles. DSMC is considered as a particle method in which one particle represents a large bulk of real gas molecules. After fulfilling all molecular movements, the collisions between molecules are simulated in each cell separately. To simulate complex flow effectively, improvements in the basic DSMC algorithm have been recently suggested by Gallis et al. [20] and Stefanov [21,22]. However, in the current work, we extend and optimize DSMC codes employed by Roohi and coworkers for simulation of a wide set of micro/nano flows [23–35]. The variable hard-sphere (VHS) model is applied as our collision model in all simulations. We use the diffuse reflection model at the solid walls. In diffuse reflection, the emission of impinging molecules is not correlated with the pre-impingement state of the molecules. The outgoing velocity of molecules is randomly assigned according to a half-range Maxwellian distribution determined by the wall temperature. Full thermal and momentum accommodation coefficients are considered for the walls. Inlet/outlet pressure boundary conditions are imposed according to the model suggested by Wang and Li [36].

It should be reminded that our DSMC solver has been optimized by different features. The cell dimensions are chosen less than mean free path, that is, smaller than $\lambda/3$ [37,38]. This criterion is implemented based on the local mean free path of cells. Each cell is subsequently divided into two subcells in each direction. The time step must be a fraction of the mean collision time and satisfy a Courant–Friedrichs–Lewy (CFL) number, based on the most probable molecular speed V_{mp}, less than one. Hadjiconstantinou [38] showed that the DSMC error exhibits quadratic dependence on the time step. He reported that for time steps of the order of "one mean free time," the error is of the order of 5 %. According to mentioned criteria, we choose the time step equal to be 0.08 of the minimum "mean free time" of all cells. Numbers of simulated particles are chosen such that there would be at least 20 particles in each cell [39]. Sampling of results starts as soon as the flow reaches to the steady state conditions. Flow sampling continues for sufficiently large time step intervals. In the beginning of the flow sampling period, flow properties were set to zero. The properties were recalculated during the new sampling period. Using this process, the effects of initial unsteady results will be eliminated and convergence of the final flow properties could be traced.

3 Results and discussions

3.1 Thermal creep concept

Thermal creep flow is an induced flow from the cold region toward the hot one. Thermal creep effect occurs only in the transitional rarefied flows, primarily along walls with a superimposed wall surface temperature gradient, see Fig. 1.

For free molecular flows, thermal creep layer fills the entire channel, creating thermal transpiration flow. Meanwhile, in the case of transitional flow, the thermal creep effects are limited to the regions near the channel's wall [8]. In this section, we evaluate the effects of thermal creep on the mass flow rate of micro/nanochannels in all ranges of Knudsen number from slip to free molecular regimes. First, we consider pure thermal creep flow through micro/nanochannels and compare the DSMC results with those of the Bhatnagar-Gross-Krook (BGK) model [19], Boltzmann-Krook-Walender (BKW) model [40], and analytical solution reported in Refs. [41,42]. At the next step, Poiseuille flow under linear wall temperature distribution will be considered.

3.2 Temperature-driven flow

Consider the channel of Fig. 2 with isobaric inlet/outlet condition. Temperature-driven force is produced via applying a linear wall temperature distribution. Channel length is 1.2 μm, and two aspect ratios (AR = L/H) of 6 and 20 are considered.

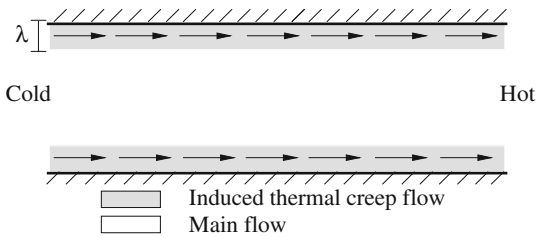

Fig. 1 Illustration of thermal creep flow induced by wall temperature gradients

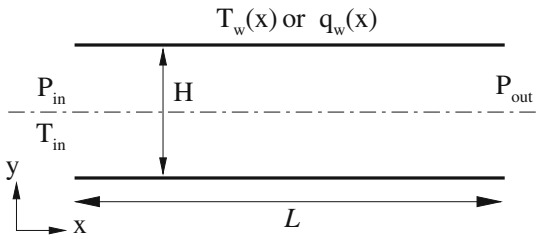

Fig. 2 Micro/nanochannel geometry and imposed boundary conditions

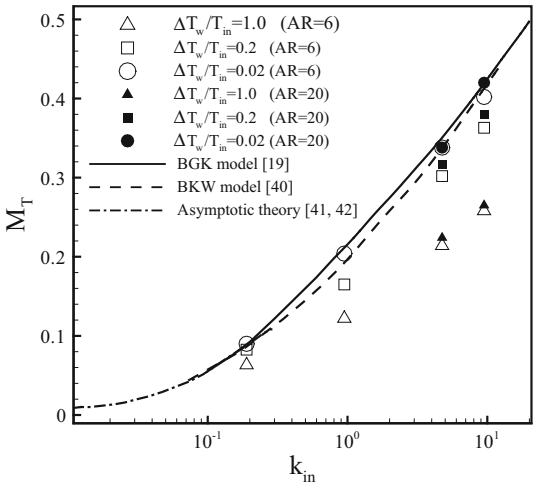

Fig. 3 The non-dimensional thermal mass flow rate versus k for the thermal transpiration flow. *White* and *block symbols* correspond to DSMC results for AR of 6 and 20, respectively

M_{T} is the non-dimensional thermal mass flow rate as follows:

$$M_{\mathrm{T}} = \frac{\dot{m}_{\mathrm{th}}}{\rho_{\mathrm{in}} \beta H \sqrt{2\mathrm{RT}_{\mathrm{in}}}} \tag{1}$$

k_{in} is defined based on the inlet Knudsen number

$$k_{\mathrm{in}} = \frac{\sqrt{\pi}}{2} \mathrm{Kn}_{\mathrm{in}} \tag{2}$$

where $\mathrm{Kn}_{\mathrm{in}} = \lambda/\mathrm{H}$ and β is defined as the non-dimensional temperature-driven force

$$\beta = \left(\frac{\Delta \mathrm{T}}{T_{\mathrm{in}}}\right)\left(\frac{H}{L}\right) \tag{3}$$

where $\Delta T = T_{\mathrm{out}} - T_{\mathrm{in}}$. Figure 3 compares the current DSMC results for non-dimensional mass flow rate with those of BGK model [19], BKW equation [40] and asymptotic theory [41,42]. The DSMC results are obtained for channels with AR values of 6 and 20. As it seen, the results for AR = 20 are closer to BGK and BKW solutions. Additionally, there is good agreement between the DSMC results and other solutions for $\Delta T_{\mathrm{w}}/T_{\mathrm{in}} = 0.02$. The deviation of the DSMC results from the BGK and BKW solutions at higher values of $\Delta T_{\mathrm{w/in}}$ is due to flow non-linearity at higher temperature gradients. In fact, BGK and BKW solutions are obtained in a linearized framework, that is, small temperature gradient is assumed. This assumption fails at small channel aspect ratios and/or high $\Delta \mathrm{T_w}/\mathrm{T_{in}}$.

In overall, the results of Fig. 3 prove the capability of the current DSMC solver to follow our target study of pressure–temperature-driven flows.

3.3 Poiseuille flows under uniform wall temperature gradient

3.3.1 Basic concept

At this stage, we consider the of thermal creep on the mass flow rate of Poiseuille flow. To achieve this, we simulate pressure-driven flows through channels with linear wall temperature distribution. To count the effects of flow rarefaction, we launch our study under different flow Knudsen numbers. Mass flow rate through micro/nano channels contains two parts as follows:

$$\dot{m} = \dot{m}_{\mathrm{p}} + \dot{m}_{\mathrm{th}} \tag{4}$$

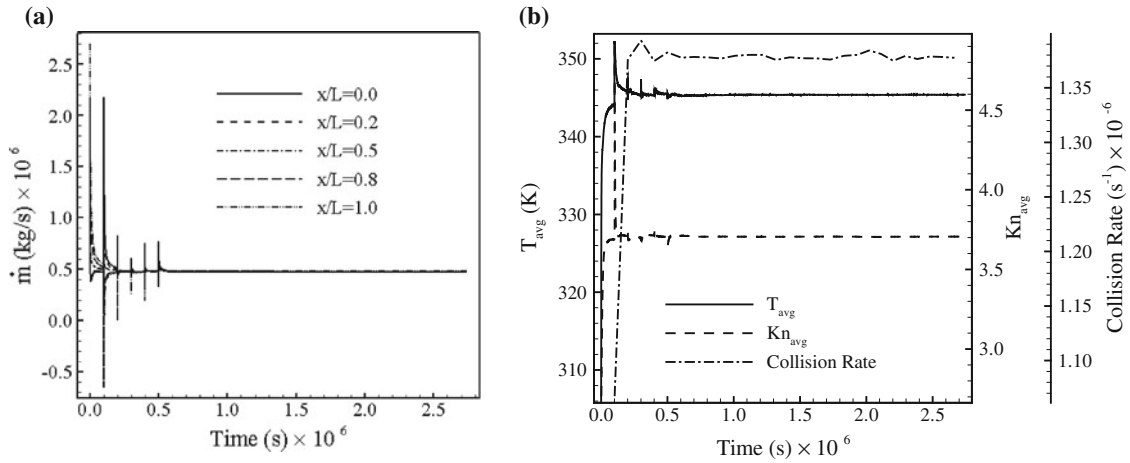

Fig. 4 Convergence behavior of the current DSMC simulations; **a** mass flow rate **b** average temperature, collision rate, average Knudsen number

where subscript "p" corresponds to pressure-driven isothermal flow, and subscripts "th" represents mass flow rate increment due to thermal creep effects.

Actually, $\dot{m}_{\mathrm{p}}$ is mass flow rate due to the inlet/outlet channel pressure difference, and $\dot{m}_{\mathrm{th}}$ is mass flow rate due to the wall temperature gradient. We consider $\dot{m}_{\mathrm{p}}$ as the mass flow rate of the pressure-driven flow with uniform wall temperature. Imposing linear wall temperature gradient, we would like to consider only the effect of wall temperature gradient under approximately zero net wall-flow heat transfer. Therefore, we set wall temperature at the first surface cell equal to the inflow temperature and keep the average wall temperature equal to the bulk temperature. This leads to a constant average Knudsen number for different values of the wall temperature gradient. At this condition, $\dot{m}_{\mathrm{th}}$ is the difference between the mass flow rates under non-zero wall temperature gradient boundary condition and the mass flow rate under uniform wall temperature boundary condition. Thermal creep leads to an induced flow from the cold region to the hot one [38]. Therefore, mass flow rate increases for streamwise wall temperature gradient and decreases for temperature gradient against stream.

3.3.2 Convergence check

Before presenting our results, it is required to ensure from the convergence of the DSMC solution. There are several possible factors to check the convergence of the DSMC simulations, that is, tracking the collision rate and averaged sampled values during the simulation. Mass flow rate is another factor for checking the convergence. Figure 4a shows the convergence behavior for crossing mass flow rate at different sections of the channel, that is, $x/L = 0.0, 0.2, 0.5$ and 1.0. Figure 4b shows average temperature, collision rate and Knudsen number variation with time. The results are taken from a test case with $\Pi = 2$, $T_{\mathrm{in}} = 300$ K, and $P_{\mathrm{in}} = 0.1$ atm. Wall temperature increases linearly from 300 to 400 K. The significant oscillation in the early stages of the solution shows the requirement for resetting the sampling process as soon as the solution reaches to the steady state condition. As it seen, after about 1.0 μs, converged DSMC solution is reached. Convergence of the mass flow rate to a constant value at different sections of the channel as well as convergence of flow properties shows that our DSMC solver is quite reliable to perform our target investigation.

3.3.3 Normalized thermal mass flow rate

Dependency on wall temperature increment

Now, we first simulate channels under an average temperature values equal to 300 K. Wall temperature values increase linearly from the inlet to the outlet, such that the average wall temperature value is equal to flow average temperature. Different levels of flow rarefaction are Kn $= 0.09, 0.37, 0.73$ and 1.46. Different Knudsen number cases are produced via changing the inlet/outlet pressure values. The effects of different levels of the wall temperature gradients are also examined. The second part is similar to part one but we set $T_{\mathrm{avg}} = 400$ K

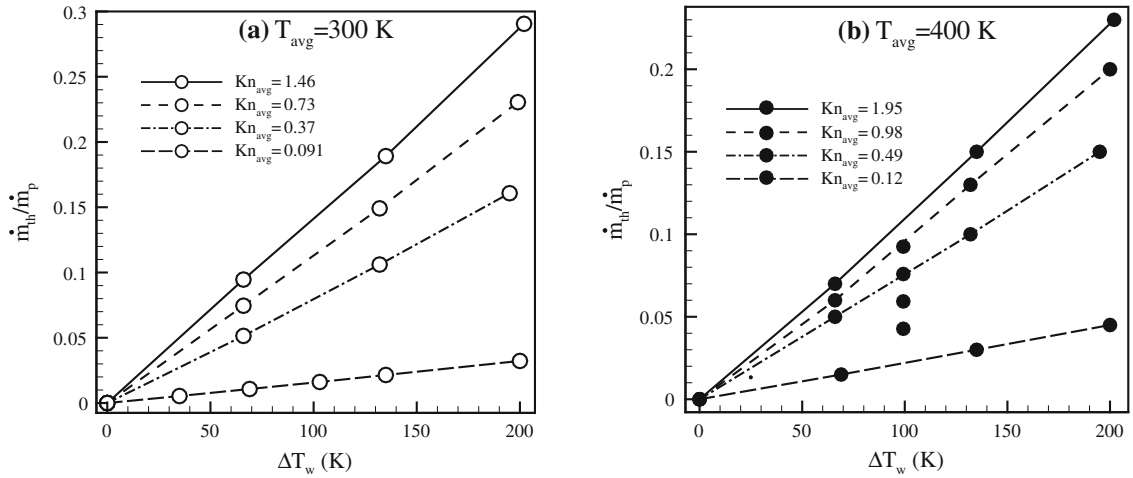

Fig. 5 Effect of wall temperature increment on the normalized thermal mass flow rate at different Knudsen numbers and bulk flow temperatures

to evaluate the effect of bulk temperature value. In the third part, we choose lower inlet/outlet pressure values to extend our studies to highly rarefied gas flows in the free molecular regime. The effects of different T_{avg} values are also considered in the third part. The inlet/outlet pressure ratio is set to $\Pi = 2$ for above three parts. To account the effects of the imposed pressure ratio, we repeat our DSMC simulations under $\Pi = 3$, 1.5, 1.2 and 1.1 in the fourth part.

Figure 5 shows the effect of wall temperature gradient values on the normalized thermal mass flow rate values. The results are obtained under different flow rarefaction conditions and streamwise wall temperature gradients, as indicated in the figure. Figure 5a, b correspond to bulk flow average temperature values of 300–400 K, respectively. The x-axis shows wall temperature increment, that is, ΔT_{w}. According to the results, thermal mass flow rate increases linearly as wall temperature gradient increases for both average temperature values. The value of $\dot{m}_{\text{p}}$ is constant through variation of the wall temperature gradient, and its value corresponds to the pressure-driven flow at zero wall temperature gradient condition. Figure 5 shows that increase in the thermal mass flow rate due to wall temperature gradient is faster for higher Knudsen numbers flows.

3.4 Dependency on Knudsen number

It is also desired to study the thermal mass flow rate behavior with the variation of the Knudsen number. For this aim, we have plotted the non-dimensional mass flux as a function of the Knudsen number in Fig. 6. Figure 6a shows the non-dimensional thermal mass flow rate as a function of the average Knudsen number at different wall temperature gradient values, that is, 70, 130 and 190 K. White and black symbols correspond to the average flow temperature values of 300–400 K, respectively. According to Fig. 6a, at a specified wall temperature gradient value, thermal mass flow rate increases as flow's average Knudsen number increases. The rate of increase is faster at lower Knudsen numbers and higher wall temperature gradient values. To make the results independent from the wall temperature gradient values, we normalize the results of Fig. 6a with respect to the wall temperature gradient values, see Fig. 6b. The results for both average temperature values of 300 K (white) and 400 K (black) have the same trend versus the Knudsen number. Consequently, we normalize graphs in this figure to their average temperature. It leads to Fig. 6c. It is well seen that both lines of Fig. 6b coalesced to the same curve in Fig. 6c.

Actually, the results given in Fig. 6c are independent from the average flow temperature and wall temperature gradient values. According to this curve, at a specified wall temperature gradient and average flow temperature values, normalized thermal mass flow rate increases as the flow rarefaction increases. This increase is slower at higher Knudsen number regimes.

We extend the results given in Fig. 6c to the free molecular regime to obtain a reliable formula for prediction of the thermal mass flow rate over a wide range of flow Knudsen number. We have performed a large set of DSMC simulations in the third part of our investigations under different conditions of flow average temperature, rarefaction and wall temperatures. Figure 7a shows the mass flow increments due to the wall temperature

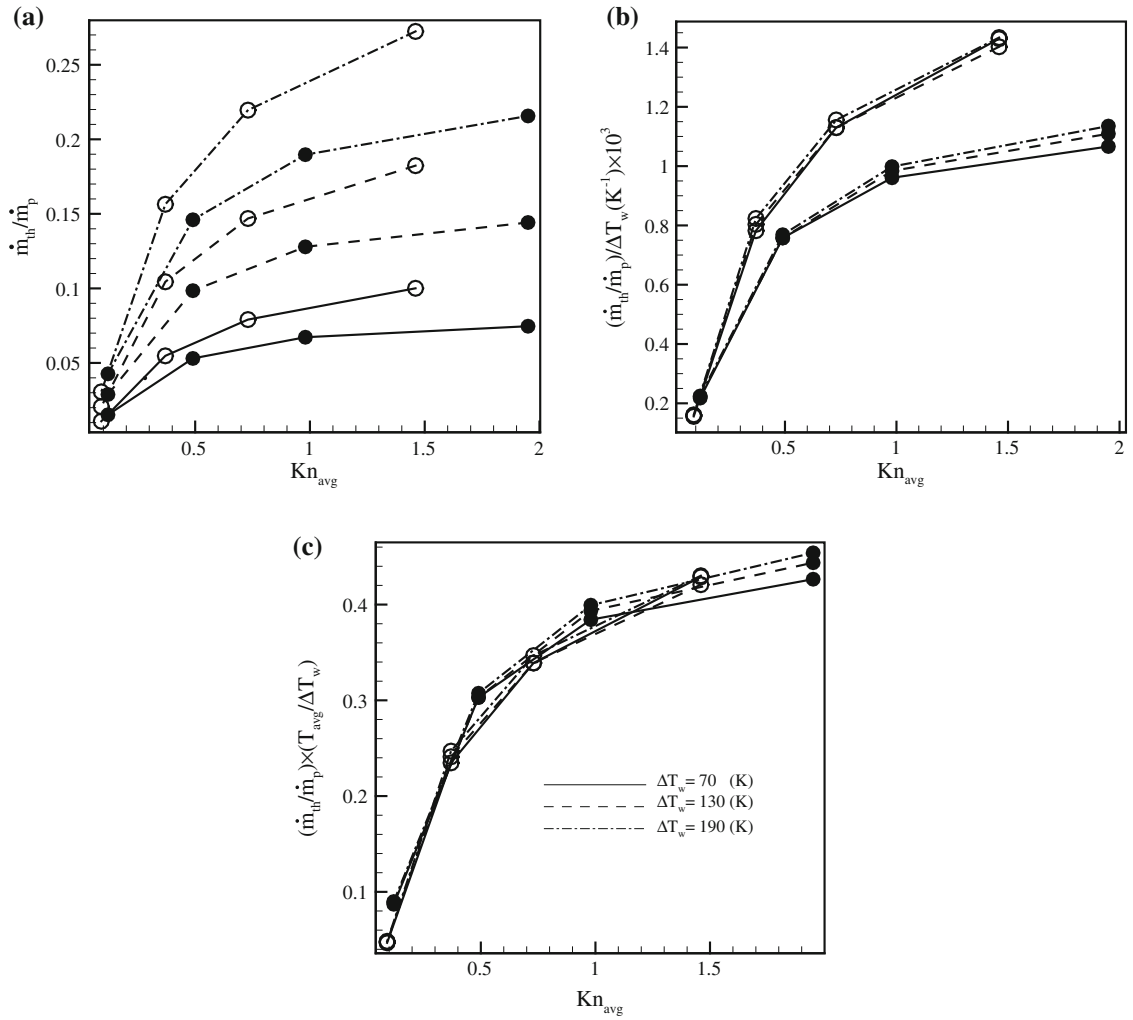

Fig. 6 Dependency of normalized thermal mass flow rate on the average Knudsen number

gradients under different values of the average flow temperature at higher values of Knudsen number. There is a linear correlation between the thermal mass flow rate and wall temperature gradient similar to that shown of in Fig. 5. Figure 7b plots the average flow Knudsen numbers for different values of T_{avg}. Each line corresponds to the same inlet/outlet boundary condition values, but symbols on each line are related to different linear wall temperature distributions. As expected, average Knudsen number is approximately constant on each line. It is because wall temperature was changed in such a way that average wall temperature is fixed to a desired T_{avg} value. This permitted us to study thermal creep effects only under different wall temperature gradient values at constant flow rarefaction.

Dependency on channel pressure ratio

We consider the effect of channel pressure ratio over a wide range of Knudsen number from slip to high transition regime, see Fig. 8. Similar to Fig. 6c, the results in Fig. 8a are independent from the flow bulk temperature and wall temperature gradient. Different pressure ratios, that are, $\Pi = 1.1, 1.2, 1.5, 2$ and 3 are applied along the channel. According to Fig. 8a, the ratio of thermal-to-pressure mass flow rate is higher for lower pressure ratio values. This indicates that the thermal creep effects are stronger under lower levels of pressure-driven force. The increase in thermal mass flow rate is more visible as Π approaches to 1. We perform a trend study to eliminate the effect of Π. Figure 8b shows the results of Fig. 8a, but independent from Π. According to this figure, the normalized thermal mass flow rate is a function of flow Knudsen number. As it seen, we could

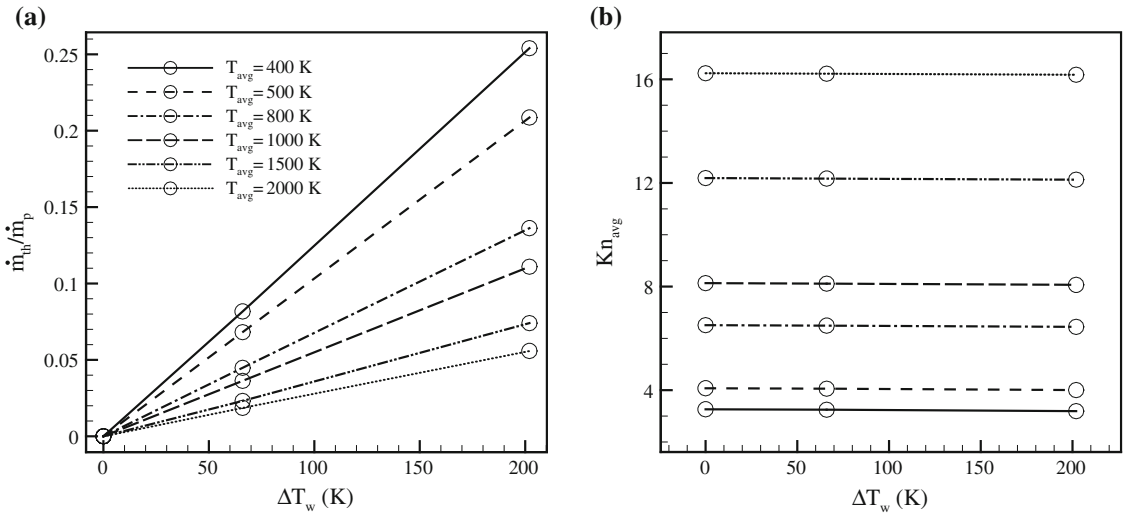

Fig. 7 **a** Investigation of normalized thermal mass flow rate at transition and free molecular regimes, **b** average Knudsen number versus wall temperature increment

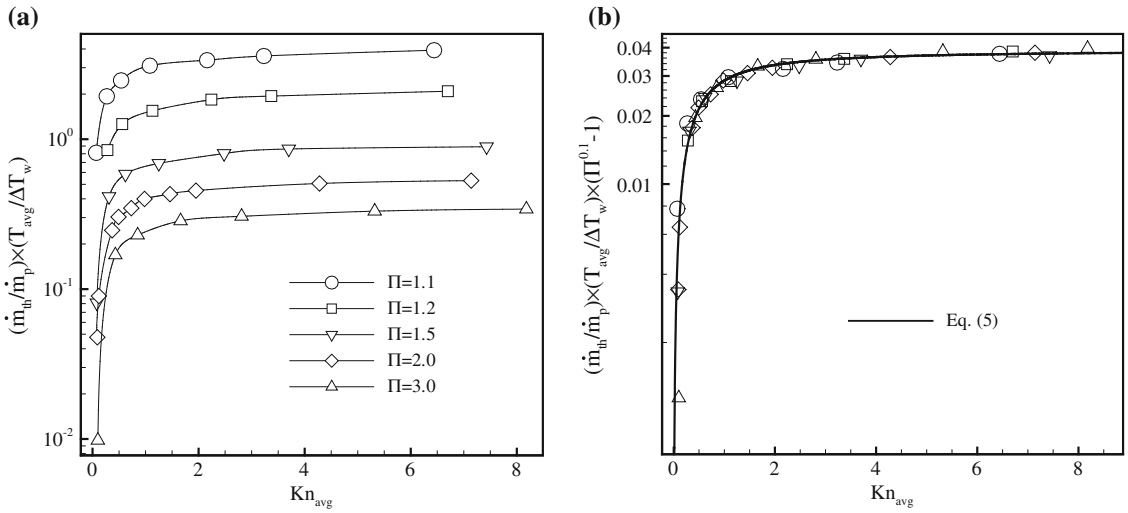

Fig. 8 Normalized thermal mass flow rate as a function of flow rarefaction, **a** results at different channel pressure ratio **b** normalized curve with respect to pressure ratio

propose a correlated formula which contains the effects of flow rarefaction, average temperature, wall temperature gradient and channel pressure ratio on the normalized thermal mass flow rate increment of the Poiseuille flow. This figure shows that the increase in the normalized thermal mass flow rate slows down as the Knudsen number increases. It reaches to a constant magnitude in the free molecular region. The curve-fitted formula to this curve is as follows:

$$\left(\frac{\dot{m}_{\mathrm{th}}}{\dot{m}_{\mathrm{p}}}\right)=\left(\frac{0.039Kn^{1.159}}{0.364+Kn^{1.159}}\right)\left(\frac{\Delta T_{\mathrm{w}}}{T_{\mathrm{avg}}}\right)/\left(\Pi^{0.1}-1\right) \tag{5}$$

According to the Fig. 8, the scaled thermal-to-pressure mass flow rate ratio increases from zero (in the case of continuum flow) to a limiting value of 0.039 at the free molecular regime, See Eq. (5). This equation represents that normalized thermal mass flow rate has a linear dependency on the normalized wall temperature increment value ($\Delta T_{\mathrm{w}}/T_{\mathrm{ave}}$) at the free molecular region. It also shows that normalized thermal mass flow rate increases as the flow rarefaction increases up to early transition regime.

Table 1 Uniform wall heat flux (UWH) cases simulated for comparison with the analytical relation (Eq. 6)

P_i (kPa)	q_w (W/m^2)	T_{avg} (K)	Kn_{out}
600	0.0	300	0.087
	-1×10^6	318	0.097
	-2×10^6	340	0.108
	-4×10^6	394	0.135
300	0.0	301	0.172
	-1×10^6	355	0.223
	-2×10^6	420	0.278
	-4×10^6	570	0.402
100	0.0	299	0.511
	-1×10^6	465	0.936
	-2×10^6	633	1.360
	-4×10^6	967	2.180

3.5 Poiseuille flows under uniform wall heat flux condition

In this section, we consider the rarefied Poiseuille flow under uniform wall heat flux (UWH) condition. First, we examine the isothermal analytical equation given by Karniadakis et al. [43] for mass flow rate prediction of Poiseuille flows under UWH conditions. Karniadakis et al. [43] derived a relation for the slip coefficient (S) using their unified slip boundary condition and their empirical relation for the viscosity coefficient. Their attempt resulted in

$$S = \frac{1}{\Pi + 1}\left[\Pi + 1 + 2\left(6\frac{2-\sigma_v}{\sigma_v} + \alpha\right)\mathrm{Kn}_{out} + 12\frac{2-\sigma_v}{\sigma_v}\frac{b+\alpha}{\Pi - 1}\mathrm{Kn}_{out}^2 \ln\left(\frac{\Pi - b\,\mathrm{Kn}_{out}}{1 - b\,\mathrm{Kn}_{out}}\right)\right] \tag{6}$$

where α and b are empirical constants whose detailed definition are provided in Ref. [43]. On the other hand, the slip coefficient (S) is defined as the normalized mass flow rate with respect to the continuum (zero Knudsen number) mass flow rate.

$$S = \frac{\dot{m}}{\dot{m}_c} \tag{7}$$

Continuum mass flow rate for a channel with length of L, height of H, pressure ratio of Π, outlet pressure of P_{out} and temperature of T is as follows:

$$\dot{m}_c = \frac{H^3 P_{out}^2}{24\mu \mathrm{LRT}}[\Pi^2 - 1] \tag{8}$$

In Eq. (8), R and μ are gas constant and viscosity coefficient, respectively. Table 1 presents the details of the numerical test cases performed for this section. For all cases, channel pressure ratio, length and aspect ratio are $\Pi = 3$, $L = 1.2\,\mu$m and AR $= 6$, respectively. Test cases are performed according to three degrees of flow rarefaction and four different values of the wall heat flux, see Table. The average flow temperature and outlet Knudsen number are also reported as output.

Figure 9 compares the results of UWH cases with the analytical equation, that is, Eq. (6), given by Karniadakis et al. [43]. In this figure, the solid lines present Eq. (6), meanwhile symbols represent the numerical results of UWH cases performed using the DSMC solver for different cases. S is obtained by normalizing the resulting mass flow rate by that of the continuum limit, $\dot{m}_c$. Values of $\dot{m}_c$ are calculated using Eq. (8) based on the parameters specified in Table 1. According to this figure, there is good agreement between the analytical equation and DSMC results in adiabatic cases. However, deviation from Eq. (6) increases as q_w values increase. The main reason is that the Eq. (6) was obtained under isothermal flow conditions with no wall heat transfer assumption. Therefore, in the case of mass flow rate prediction of Poiseuille flows under UWH condition, analytical relation given by Eq. (6) is suitable only for adiabatic walls. In non-zero wall heat flux cases, S is underestimated with respect to Eq. (6). As the magnitude of wall heat flux increases, that is, stronger heating, deviation from Eq. (6) increases.

At this step, we would like to examine the derived correlation, Eq. (5), in prediction of mass flow rate of UWH cases. For this aim, we had set up a number of test cases in which Poiseuille flow is analyzed under

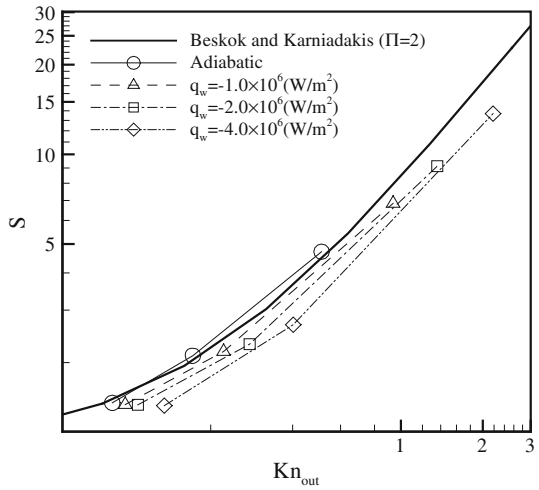

Fig. 9 Comparison of slip coefficient of channel flow under UWH condition with the analytical relation (Eq. 6)

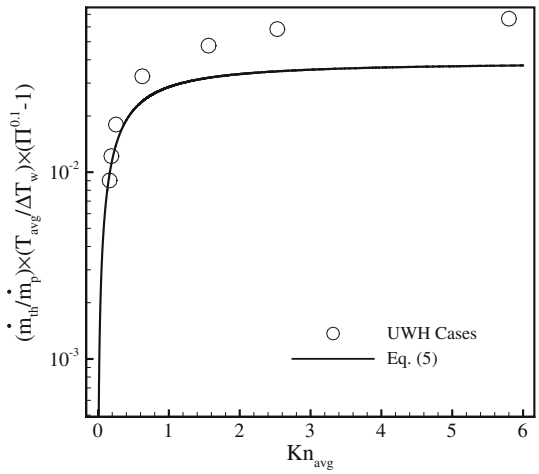

Fig. 10 Comparison of normalized thermal mass flow rate of "uniform wall heat flux (UWH)" cases with the correlated formula (Eq. 5)

UWH condition. Corresponding isothermal cases were also simulated to consider the thermal creep effects due to imposed uniform wall heat flux conditions. The details of test cases for both of UWH and of UWT cases are reported in Table 2. The pressure ratio is set to 3 for all cases. Each UWT case is actually a pressure-driven flow in which inflow and wall temperature values are equal to the average flow temperature in corresponding UWH case.

Figure 10 compares the results for UWH cases with Eq. (5). Mass flow rates obtained from UWT and UWH cases are presented by $\dot{m}_\mathrm{p}$ and $\dot{m}$, respectively. The thermal mass flow rate $\dot{m}_\mathrm{th}$ is obtained by subtraction of $\dot{m}_\mathrm{p}$ from $\dot{m}$. According to this figure, there is good agreement between the UWH cases with Eq. (5) for Knudsen numbers less than 0.5. However, the differences increase as flow rarefaction increases. The reason is that the Eq. (5) is obtained under zero net wall-flow heat transfer, while there are non-zero wall heat flux values in UWH cases. These non-zero q_w values affect the flow physics. This effect also can be found by investigating flow rarefactions given in Table 2, where the flow average Knudsen number values are different for both UWT and UWH cases at higher flow rarefaction or higher values of q_w. However, Eq. (5) could be used to predict the mass flow rate in the case of uniform wall heat flux conditions for average Knudsen numbers less than 0.5, that is, early transition regime.

Table 2 Uniform wall heat flux (UWH) cases and corresponding uniform wall temperature (UWT) cases simulated for comparing the results with Eq. (5)

UWH cases				UWT cases
P_{in} (Pa)	q_w (W/m^2)	T_{avg} (K)	Kn_{avg}	Kn_{avg}
3.0×10^5	-1×10^6	347	0.162	0.162
3.0×10^5	-2×10^6	400	0.188	0.187
3.0×10^5	-4×10^6	533	0.247	0.253
1.0×10^5	-1×10^6	449	0.625	0.642
0.5×10^5	-1×10^6	566	1.500	1.633
0.2×10^5	-1×10^5	357	2.500	2.570
0.2×10^5	-1×10^6	896	5.160	6.430

4 Conclusions

We present a mass flow rate study for pressure–temperature-driven flows through micro/nanoscale channels using DSMC method. Temperature-driven forces were generated via applying a non-uniform wall temperature distribution. The effects of thermal creep studied over a wide range of flow rarefaction from the slip to free molecular regime, and an analytical expression for normalized thermal mass flow rate is suggested. Our results showed that the normalized thermal mass flow rate approaches to a value of 0.039 at the free molecular limit. Our suggested analytical expression is a function of Knudsen number, normalized wall temperature increment and pressure ratio. Next, we examine our formula for Poiseuille flows under uniform wall heat flux conditions. Our studies showed that formula could be used for mass flow rate prediction of Poiseuille flows under UWH conditions at Knudsen numbers less than 0.5. We also showed that using standard analytical relations for mass flow rate of Poiseuille flows under adiabatic walls is still fair. For higher values of the Knudsen number, wall-flow heat transfer leads to deviation from the standard formula. The reason is that the effect of heat addition to the flow is more effective in flows with higher degrees of rarefaction.

Acknowledgments The authors would like to acknowledge the financial supports provided by the Faculty of Engineering, Ferdowsi University of Mashhad under Grant No. 18888/2.

References

1. Taylor, J., Ren, C.L.: Application continuum mechanics to fluid flow in nanochannels. Microfluid. Nanofluid. **1**(4), 356 (2005)
2. Ho, C.M., Tai, Y.C.: Micro-electro-mechanical-system (MEMS) and fluid flows. Annu. Rev. Fluid Mech. **30**, 579 (1998)
3. Cercignani, C.: The Boltzmann Equation and its Applications. Springer, New York (1988)
4. Bird, G.A.: Molecular Gas Dynamics and the Direct Simulation of Gas Flows. Oxford Science, Oxford (1994)
5. Taheri, P., Struchtrup, H.: Rarefaction effects in thermally-driven microflows. Physica A **389**, 3069 (2010)
6. Sone, Y., Waniguchi, Y., Aoki, K.: One-way flow of a rarefied gas induced in a channel with a periodic temperature distribution. Phys. Fluids **8**(8), 2227 (1996)
7. Alexeenko, A.A., Gimelshein, S.F., Muntz, E.P., Ketsdever, A.D.: Kinetic modeling of temperature driven flows in short microchannels. Int. J. Thermal Sci. **45**, 1045 (2006)
8. Han, Y.L., Muntz, E.P., Alexeenko, A., Young, M.: Experimental and computational studies of temperature gradient-driven molecular transport in gas flows through nano/microscale channels. Nanoscale Microscale Thermophys. Eng. **11**, 151 (2007)
9. Han, Y.L.: Thermal-creep-driven flows in Knudsen compressors and related nano/microscale gas transport channels. J. Microelectromech. Syst. **17**(4), 984–997 (2008)
10. Sone, Y.: Kinetic Theory and Fluid Dynamics. Birkhäuser, Boston (2002)
11. Knudsen, M.: Eine Revision der Gleichgewichtsbedingung der Gase. Thermische Molekularströmung. Ann. Phys. **31**, 205 (1910)
12. Knudsen, M.: Thermischer Molekulardruck der Gase in Röhren. Ann. Phys. **33**, 1435 (1910)
13. Loyalka, S.K.: Kinetic theory of thermal transpiration and mechanocaloric effect. I. J. Chem. Phys. **55**(9), 4497 (1971)
14. Loyalka, S.K.: Slip in the thermal creep flow. Phys. Fluids **14**(1), 21 (1971)
15. Loyalka, S.K.: Kinetic theory of thermal transpiration and mechanocaloric effect. II. J. Chem. Phys. **63**(9), 4054 (1975)
16. Loyalka, S.K., Storvick, T.S.: Kinetic theory of thermal transpiration and mechanocaloric effect. III. Flow of a polyatomic gas between parallel plates. J. Chem. Phys. **71**(1), 339 (1979)
17. Lo, S.S., Loyalka, S.K., Storvick, T.S.: Kinetic theory of thermal transpiration and mechanocalorlc effect. V. Flow of polyatomic gases in a cylindrical tube with arbitrary accommodation at the surface. J. Chem. Phys. **81**(5), 2439 (1984)
18. Kanki, T., Iuchi, S.: Poiseuille flow and thermal creep of a rarefied gas between parallel plates. Phys. Fluids **16**(5), 594 (1973)
19. Ohwada, T., Sone, Y., Aoki, K.: Numerical analysis of the Poiseuille and thermal transpiration flows between two parallel plates on the basis of the Boltzmann equation for hard-sphere molecules. Phys. Fluids A **1**(12), 2042 (1989)

20. Gallis, M.A., Torczynski, J.R., Rader, D.J., Bird, G.A.: Convergence behavior of a new DSMC algorithm. J. Comput. Phys. **228**, 4532 (2009)
21. Stefanov, S.: Particle Monte Carlo algorithms with small number of particles in grid cells. In: Numerical Methods and Applications. Lecture Notes in Computer Science, vol. 6064, p. 110 (2010)
22. Stefanov, S.: On DSMC calculations of rarefied gas flows with small number of particles in cells. SIAM J. Sci. Comput. **33**, 677 (2011)
23. Roohi, E., Darbandi, M.: Extending the Navier–Stokes solutions to transition regime in two-dimensional micro- and nanochannel flows using information preservation scheme. Phys. Fluids **21**, 082001 (2009)
24. Roohi, E., Darbandi, M., Mirjalili, V.: Direct simulation Monte Carlo solution of subsonic flow through micro/nanoscale channels. J. Heat Transf. **131**, 92402 (2009)
25. Scanlon, T.J., Roohi, E., White, C., Darbandi, M., Reese, J.M.: An open source, parallel DSMC code for rarefied gas flows in arbitrary geometries. Comput. Fluids **39**, 2078 (2010)
26. Darbandi, M., Roohi, E.: Study of subsonic/supersonic gas flow through micro/nanoscale nozzles using unstructured DSMC solver. Microfluid. Nanofluid. **10**, 321 (2011)
27. Darbandi, M., Roohi, E.: DSMC simulation of subsonic flow through nanochannels and micro/nano steps. Int. Commun. Heat Mass Transf. **38**(10), 1444–1449 (2011)
28. Roohi, E., Darbandi, M.: Recommendations on performance of parallel DSMC algorithm in solving subsonic nanoflows. Appl. Math. Model. **36**, 2314–2321 (2012)
29. Ejtehadi, O., Roohi, E., Abolfazli, J.: Investigation of basic molecular gas structure effects on hydrodynamics and thermal behaviors of rarefied shear driven flow using DSMC. Int. Commun. Heat Mass Transf. **39**(3), 439–448 (2012)
30. Akhlaghi, H., Roohi, E., Stefanov, S.: A new iterative wall heat flux specifying technique in DSMC for heating/cooling simulation at micro/nanoscales, vol. 56, pp. 111–125 (2012)
31. Abolfazli, J., Ejtehadi, O., Roohi, E.: Second law analysis of micro/nano Couette flow using DSMC. Int. J. Exergy (2012) (accepted)
32. Roohi, E., Akhlaghi, H.: Study of physical aspects of rarefied gas flow through micro/nano scale channels using DSMC. Arabian J. Sci. Eng. (2012) (accepted)
33. Darbandi, M., Roohi, E.: Applying a hybrid DSMC/Navier–Stokes frame to explore the effect of splitter plates in micro/nano propulsion systems. Sens Actuators A Phys **189**, 409–419 (2013)
34. Mohammadzadeh, A., Roohi, E., Niazmand, H., Stefanov, S., Myong, R.S.: Detailed investigation of thermal and hydrodynamic behaviour in micro/nano cavity using DSMC. Phys. Rev. E **85**, 056305 (2012)
35. Mohammadzadeh, A., Roohi, E., Niazmand, H.: A parallel DSMC investigation of monatomic/diatomic gas flows in micro/nano cavity. Numer. Heat Transf. Part A Appl. **63**(4), 305–325 (2013)
36. Wang, M., Li, Z.: Simulations for gas flows in microgeometries using the direct simulation Monte Carlo method. Int. J. Heat Fluid Flow **25**, 975 (2004)
37. Alexander, F.J., Garcia, A.L., Alde, B.J.: Cell size dependence of transport coefficients in stochastic particle algorithms. Phys. Fluids **10**(6), 1540 (1998)
38. Hadjiconstantinou, N.G.: Analysis of discretization in the direct simulation Monte Carlo. Phys. Fluids **12**(10), 2634 (2000)
39. Shu, C., Mao, X.H., Chew, Y.T.: Particle number per cell and scaling factor effect on accuracy of DSMC simulation of micro flows. Int. J. Numer. Methods Fluids **15**(8), 827 (2005)
40. Loyalka, S.K.: Comments on Poiseuille flow and thermal creep of a rarefied gas between parallel plates. Phys. Fluids **17**(5), 1053 (1974)
41. Ohwada, T., Sone, Y., Aoki, K.: Numerical analysis of the shear and thermal creep flows of a rarefied gas over a plane wall on the basis of the linearized Boltzmann equation for hard-sphere molecules. Phys. Fluids AI **1**(9), 1588 (1989)
42. Sone, Y., Aoki, K.: Asymptotic theory of slightly rarefied gas flow and force on a closed body. Mem. Fac. Eng., Kyoto Univ. **49**, 237–248 (1987)
43. Karniadakis, G.E., Beskok, A., Aluru, N.: Microflows and Nanoflows: Fundamentals and Simulation. Springer, New York (2005)